Defect modes and transmission properties of left-handed bandgap structures

Ilya V. Shadrivov,[1] Nina A. Zharova,[1,2] Alexander A. Zharov,[1,3] and Yuri S. Kivshar[1]
[1]*Nonlinear Physics Centre and Centre for Ultra-high Bandwidth Devices for Optical Systems (CUDOS), Research School of Physical Sciences and Engineering, Australian National University, Canberra, Australian Capital Territory 0200, Australia*
[2]*Institute of Applied Physics, Russian Academy of Sciences, Nizhny Novgorod 603600, Russia*
[3]*Institute for Physics of Microstructures, Russian Academy of Sciences, Nizhny Novgorod 603950, Russia*
(Received 16 February 2004; revised manuscript received 5 May 2004; published 29 October 2004)

We analyze transmission of electromagnetic waves through a one-dimensional periodic layered structure consisting of slabs of a left-handed metamaterial and air. We derive the effective parameters of the metamaterial from a microscopic structure of wires and split-ring resonators possessing the left-handed characteristics in the microwave frequency range, and then study, by means of the transfer-matrix approach and the finite-difference time-domain numerical simulations, the transmission properties of this layered structure in a band gap associated with the zero averaged refractive index. By introducing defects, the transmission of such a structure can be made tunable, and we study the similarities and differences of the defects modes excited in two types of the band gaps.

DOI: 10.1103/PhysRevE.70.046615 PACS number(s): 42.70.Qs, 41.20.Jb, 78.20.−e

I. INTRODUCTION

Electromagnetic materials with both negative dielectric permittivity and negative magnetic permeability have been discussed theoretically a long time ago by Veselago [1] as a hypothetical material termed "left handed" because the wave vector creates a left set of vectors with the electric and magnetic fields. Many unusual properties of the left-handed materials such as negative refraction can be associated with their negative refractive index, as has been demonstrated for microwaves by several reliable experiments for the metamaterials created by a lattice of split-ring resonators and wires [2,3] and numerical finite-difference time-domain (FDTD) simulations (see, e.g., Ref. [4], and references therein).

Multilayered structures that include left-handed materials (or, in general, materials with negative refraction) can be considered as a sequence of the flat lenses that provide an optical cancellation of the layers with positive refractive index leading to either enhanced or suppressed transmission [5–7]. More importantly, a one-dimensional stack of layers with alternating positive and negative-refraction materials with zero averaged refractive index displays an unusual transmission band gap [6,8–11] near the frequency where the condition $\langle n\rangle = 0$ is satisfied; such a band gap is quite different from a conventional Bragg reflection gap because it appears due to different physics of wave reflection. In particular, the periodic structures with zero averaged refractive index demonstrate a number of unique properties of the beam transmission observed as strong beam modification and reshaping [10] being also insensitive to disorder that is symmetric in the random variable [8].

In this paper, we study transmission properties of a multilayer periodic stack (also called one-dimensional photonic crystal or photonic bandgap structure) created by alternating slabs of two types of materials, with positive and negative refractive indices. We also consider the same structure with an embedded defect and take into account realistic parameters of the metamaterials such as dispersion and losses. In spite of the fact that our calculations are presented for the metamaterials with the left-handed properties in the microwave domain, many of our results are rather general and they can be also useful for other types metamaterials [12,13], including not yet demonstrated materials operating at THz or even optical wavelengths.

We consider a band-gap structure schematically shown in Fig. 1. First, in Sec. II we study the properties of the left-handed material as a composite structure made of arrays of wires and split-ring resonators (see the inset in Fig. 1) and derive the general results for the effective dielectric permittivity and magnetic permeability. Second, we study the transmission of electromagnetic waves through the layered structure consisting of alternating slabs of composite left-handed metamaterial using the calculated effective parameters (see Sec. III). We assume that the structure includes a defect layer (see Fig. 1) that allows tunability of the wave transmission near the defect frequency. Using the transfer-matrix method, we describe the defect-induced localized states in such a structure and reveal that the defect modes may appear in different parameter regions and for both $\langle n\rangle = 0$ and Bragg scattering band gaps. Depending on the defect parameters, the maximum transmission can be observed in all or just some spectral band gaps of the structure. We demonstrate that the frequency of the defect mode is less sensitive to

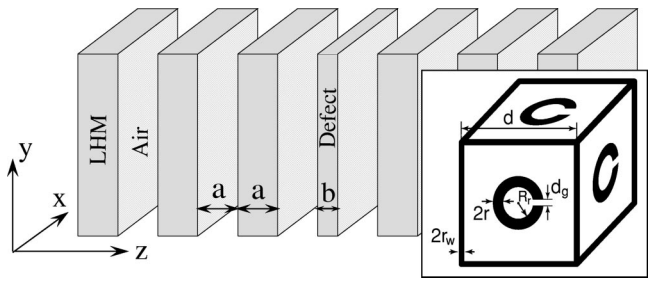

FIG. 1. Schematic picture of a multilayered structure consisting of alternating metamaterial slabs and air. The inset shows the unit cell of the metallic SRR-wire metamaterial.

manufacturing disorder for the larger defect layer. In Sec. IV we present the results of our two-dimensional FDTD numerical simulations based on the microscopic parameters of the left-handed material and also study the spatiotemporal evolution of the transmitted and reflected fields. Finally, in Sec. V we summarize our findings.

II. METAMATERIAL CHARACTERISTICS

We assume that the metamaterial that displays left-handed characteristics at microwaves is created by a three-dimensional lattice of wires and split-ring resonators (SRRs), as shown schematically in the inset of Fig. 1. According to the derivation presented in Refs. [14,15], the main contribution to the effective dielectric permittivity of this structure is given mainly by the wires, whereas the magnetic response is determined by SRRs. Although a three-dimensional lattice of wires contains closed circuits, we neglect their contribution to the magnetic permeability, because this effect is nonresonant and, therefore, it is weak. The effective dielectric permittivity of such a structure can be derived in a consistent way [14,15], and it can be written in the form

$$\epsilon(\omega) = 1 - \frac{\omega_p^2}{\omega(\omega - i\gamma_\epsilon)}, \tag{1}$$

where $\omega_p \approx (c/d)[2\pi/\ln(d/r_w)]^{1/2}$ is the effective plasma frequency $\gamma_\epsilon = c^2/2\sigma S\ln(d/r_w)$, σ is the wire conductivity, S is the effective cross section of a wire, $S=\pi r_w^2$, for $\delta > r_w$, and $S \approx \pi\delta(2r-\delta)$, for $\delta < r_w$, where $\delta = c/\sqrt{2\pi\sigma\omega}$ is the skin-layer thickness.

To calculate the effective magnetic permeability of the lattice of SRRs, we write its magnetization M in the form (see also Ref. [16])

$$M = (n_m/2c)\pi R_r^2 I_r, \tag{2}$$

where $n_m = 3/d^3$ is the number of SRRs per unit cell, R_r is the SRR radius (see the inset in Fig. 1), I_r is the current in the SRR. We assume that SRR is an effective oscillatory circuit with inductance L and resistance R of the wire, and capacity C of the SRR slot. In this circuit the electromotive force $\mathcal{E}$ appears due to an alternating magnetic field of the propagating wave. Under these assumptions, the evolution of the current I_r in single SRR is governed by the equation

$$L\frac{d^2 I_r}{dt^2} + R\frac{dI_r}{dt} + \frac{1}{C}I_r = \frac{d\mathcal{E}}{dt}, \tag{3}$$

with

$$\mathcal{E} = -\frac{\pi R_r^2}{c}\frac{dH'}{dt},$$

where H' is the acting (microscopic) magnetic field, which differs from the averaged (macroscopic) magnetic field. We describe the SRR array as a system of magnetic dipoles, which is valid when the number of SRRs in the volume λ^3 is big enough, and use the Lorenz-Lorentz relation between the microscopic and macroscopic magnetic fields [17]

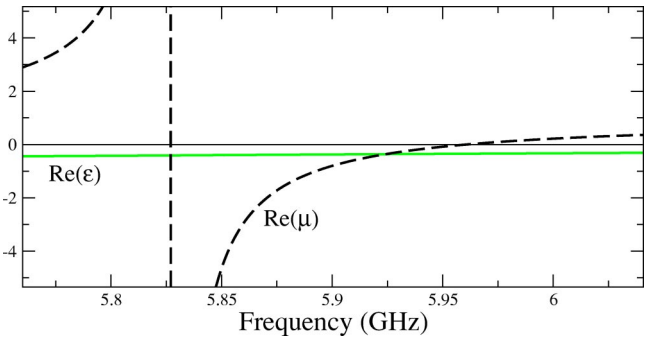

FIG. 2. (Color online). Real part of the dielectric permittivity Re(ϵ) shown by solid lines, and the real part of magnetic permeability Re(μ), shown by dashed lines, for a lattice of metallic SRRs and wires.

$$H' = H + \frac{4\pi}{3}M = B - \frac{8\pi}{3}M. \tag{4}$$

As a result, from Eqs. (2)–(4) we obtain the effective magnetic permeability of the structure in the form

$$\mu(\omega) = 1 + \frac{F\omega^2}{\omega_0^2 - \omega^2(1+F/3) + i\omega\gamma}, \tag{5}$$

where $F = 2\pi n_m(\pi R_r^2/c)^2/L$, $\omega_0^2 = 1/LC$, and $\gamma = R/L$. Inductance L, resistance R, and capacitance C are given by the following results (see, e.g., Ref. [18]):

$$L = \frac{4\pi R_r}{c^2}\left[\ln\left(\frac{8R_r}{r}\right) - \frac{7}{4}\right],\ R = \frac{2\pi R_r}{\sigma S_r},\ C = \frac{\pi r^2}{4\pi d_g},$$

where r is the radius of the wire that makes a ring, σ is conductivity of the wire, S_r is the effective area of the cross-section of the SRR wire defined similar to that of a straight wire, and d_g is the size of the SRR slot. We note, that the result for C should hold provided $d_g \ll r$.

We take the parameters of a metallic SRR-wire composite as $d=1$ cm, $r_w=0.05$ cm, $R_r=0.2$ cm, $r=0.02$ cm, $d_g = 10^{-3}$ cm, and its conductivity as $\sigma = 2\times 10^{19}$ s^{-1}, and calculate the effective frequency dependencies of permittivity $\epsilon(\omega)$ and permeability $\mu(\omega)$ according to Eqs. (1) and (5), respectively, and show these dependencies in Fig. 2. The resonance frequency appears near 5.82 GHz, and the region of the simultaneously negative ϵ and negative μ is located between the frequencies 5.82 and 5.96 GHz. The imaginary part of the magnetic permeability, which determines the effective losses in a left-handed material, is larger near the resonance.

III. TRANSMISSION AND DEFECT MODES

Now we consider a periodic layered structure created by a system of seven left-handed dielectric slabs of the width a separated by air, as shown in Fig. 1. The number of slabs is chosen to keep losses in the structure at a reasonably low level, still having visible effects of periodicity. The middle layer of the left-handed material is assumed to have a different thickness, $b = a(1+\Delta)$, becoming a structural defect.

To study the transmission characteristics of such a periodic layered structure, we consider the scattering of a normal-incidence plane wave described by the Helmholtz-type equation for the scalar electric field

$$\left[\frac{d^2}{dz^2}+\frac{\omega^2}{c^2}\epsilon(z)\mu(z)-\frac{1}{\mu(z)}\frac{d\mu}{dz}\frac{d}{dz}\right]E=0, \tag{6}$$

where $\epsilon(z)$ and $\mu(z)$ are the dielectric permittivity and magnetic permeability of a bulk material.

First, we study the corresponding *infinite* structure without defects and calculate its bandgap transmission spectrum. In an infinite periodic structure, propagating waves have the form of the Floquet-Bloch modes satisfying the periodicity condition, $E(z+2a)=E(z)\exp(2iaK_b)$, where K_b is the Bloch wave number. Possible values of K_b are found as solutions of the standard eigenvalue equation for a two-layer periodic structure, as discussed in detail in Ref. [11],

$$2\cos(K_b 2a)=2\cos[(k_r+k_l)a]-\left(\frac{p_r}{p_l}+\frac{p_l}{p_r}-2\right)\times\sin(k_r a)\sin(k_l a), \tag{7}$$

where $p_r=1$, $p_l=\sqrt{\epsilon/\mu}$, $k_r=\omega/c$, and $k_l=\sqrt{\epsilon\mu}\omega/c$ are the wave vectors in air and left-handed slabs, respectively. For real values of K_b, the Bloch waves are propagating; complex values of K_b indicate the presence of band gaps, where the wave propagation is suppressed. The spectral gaps appear when the argument of the cosine function in Eq. (7) becomes the whole multiple of π, and no real solutions for K_b exist. These gaps are usually termed as Bragg gaps. The presence of the left-handed material in the structure makes it possible for the argument to vanish, so that the wave propagation becomes prohibited in this case as well, thus creating an additional band gap, which do not exist in conventional periodic structures. As a matter of fact, the condition $|k_r|=|k_l|$ corresponds to the zero average refractive index $\langle n\rangle=0$, as discussed in Refs. [6,8–11]. However, the inherent feature of the left-handed materials is their frequency dispersion, so that the condition $|k_r|=|k_l|$ defines a characteristic frequency ω^* at which the indices of refraction in both the media compensate each other. In a sharp contrast to the conventional Bragg reflection gaps, the position of this additional $\langle n\rangle=0$ gap in the frequency domain does not depend on the optical period of the structure.

For the parameters of the left-handed composite media described above, the critical frequency ω^*, at which the average refractive index of the structure vanishes, is found as $\omega^*\approx 2\pi 5.8636\times 10^9\ \mathrm{s}^{-1}$. Importantly, the transmission coefficient calculated at the frequency $\omega=\omega^*$ for the seven-layer structure shows a characteristic resonant dependence as a function of the normalized slab thickness a/λ, where $\lambda=2\pi c/\omega^*$, as shown in Fig. 3. The transmission maxima appear in the gap $\langle n\rangle=0$, when the slab thickness a coincides with a whole multiple of a half of the wavelength. The width of the transmission peaks decreases with the number of left-handed layers in the structure. The transmission maxima decrease with increasing thickness of the structure due to losses

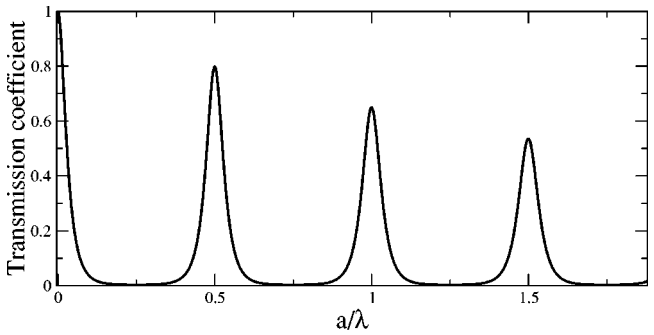

FIG. 3. Transmission coefficient of a finite periodic structure created by seven layers of the left-handed metamaterial vs the normalized thickness of the slab a/λ, where $\lambda=2\pi c/\omega^*$ and the frequency $\omega=\omega^*$ corresponds to the condition $\langle n\rangle=0$.

in the left-handed material which become larger for thicker slabs. One of the interesting features of the novel gap defined by the condition $\langle n\rangle=0$ is that the transmission coefficient *can vanish even for very small values of the slab thickness*. This property can be employed to create effective mirrors in the microwave frequency range operating in this novel $\langle n\rangle=0$ gap which can be effectively thinner than the wavelength of electromagnetic waves.

The transmission coefficient of a finite periodic structure formed by seven layers of the left-handed metamaterial is shown in Figs. 4(a) and 4(b) as a function of the frequency,

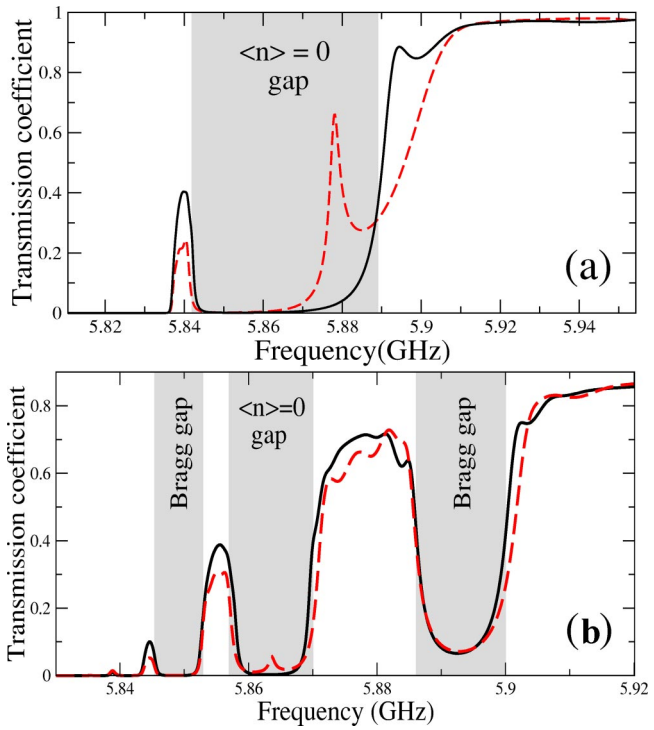

FIG. 4. (Color online). Transmission coefficient of a finite periodic structure created by seven layers of the left-handed metamaterial vs the incident wave frequency. (a) The structure with the period $a=0.25\lambda$, without (solid) and with (dashed) defect layer ($\Delta=-0.8$). (b) The structure with the period $a=1.25\lambda$ without (solid) and with (dashed) defect layer ($\Delta=-0.6$).

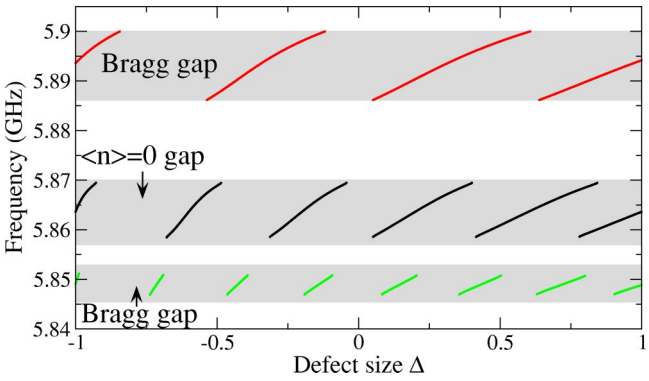

FIG. 5. (Color online). Spectrum of the defect-mode frequencies vs the normalized size of the defect Δ in the left-handed bandgap structure with the period $a=1.25\lambda$.

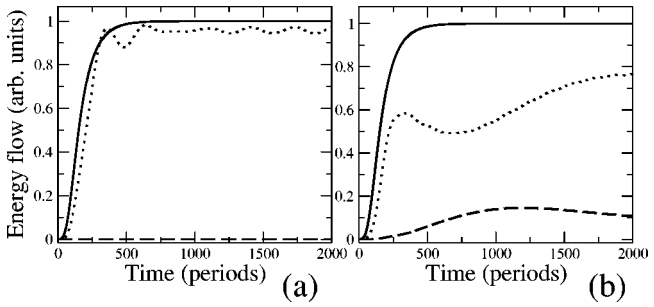

FIG. 6. Numerical FDTD simulation results showing relaxation processes in a band-gap structure with a defect. Solid: incident energy flow, dashed: transmitted energy flow, dotted: reflected energy flow. The parameters are: $a=0.25\lambda$, $\Delta=-0.8$. (a) Defect mode is not excited, $\omega=2\pi\times5.86\times10^9$ s^{-1}. (b) Defect mode is excited, $\omega=2\pi\times5.878\times10^9$ s^{-1}.

for two structures that differ by the period a. For the quarter-wavelength slabs [see Fig. 4(a)], the only visible band gap is the novel gap $\langle n\rangle=0$ centered near the frequency ω^*. When this periodic structure includes a defect, the transmission peak associated with the excitation of the defect mode is observed inside the $\langle n\rangle=0$ gap, as shown by a dashed curve. For the structure with thicker slabs, e.g., for the structure with the period $a=1.25\lambda$ [see Fig. 4(b)], the $\langle n\rangle=0$ gap becomes narrower but it remains centered near the frequency ω^*. The transmission coefficient of this latter bandgap structure shows, in addition to the $\langle n\rangle=0$ gap, two Bragg scattering gaps. Due to the increased losses in this second type of the bandgap structure where the slabs are thicker than those in the structure corresponding to Fig. 4(a), the effects of the resonant transmission at the defect mode become less visible. Moreover, for the parameters considered here the defect mode appears only in the $\langle n\rangle=0$ gap, whereas it does not appear in the Bragg gaps. For larger thickness of the slabs, higher-order Bragg gaps may appear in the frequency range where the composite material possesses left-handed properties.

In Fig. 5, we show the spectrum of the defect-mode frequencies for the layered structure with the period $a=1.25\lambda$ as a function of the normalized size of the defect Δ. We notice a number of important features, which can also be found for other types of such left-handed structures. First of all, the defect modes do not always appear simultaneously in all gaps of the spectrum and, therefore, they can be placed selectively either in the Bragg gaps or the zero-index gap. Second, the slope of the curves in Fig. 5 decreases with the thickness of the defect layer. As a result, the eigenfrequencies of the modes supported by a thicker defect layer can be more tolerant to disorder introduced by manufacture. These features of the defect modes excited in the zero-index gap may be important for engineering tunable properties of the layered structures with negative refraction. In particular, the existence of different types of the defect modes allow to access different types of band gaps independently.

IV. NUMERICAL SIMULATIONS

In order to analyze the spatiotemporal evolution of the transmitted fields and the beam scattering under realistic conditions, we perform two-dimensional finite-difference time-domain (FDTD) numerical simulations of the beam propagation through the left-handed periodic structure of seven layers with a defect. We would like to point out that the time-resolved numerical simulations are performed in order to estimate the characteristic time of the defect mode excitation, which can determine the operation time of such a multilayer structure. This issue seems to be important because the novel type of the band gap discussed in this paper is based on a different physical mechanism of the transmission cancellation, and it requires the vanishing *averaged* refractive index.

In the FDTD simulations, we consider the TM-polarized Gaussian beam of the width 20λ propagating normal to the layered structure with the period $a=0.25\lambda$; the considered periodic structure corresponds to the transmission coefficient shown in Fig. 4(a) by a dashed line. The boundaries of the simulation area are perfectly matched layers (PML's), so that no reflection from the boundaries takes place. The slabs of the left-handed material do not extend to the PML boundaries, since the layer is perfectly matched to the air space only. The mesh of the numerical simulation area is 100×800 points in the transverse and propagation directions, respectively.

First, we choose the carrier frequency of the incident field in the $\langle n\rangle=0$ gap. The temporal evolution of the energy flows (Poynting vector integrated over the transverse dimension) for the incident, transmitted, and reflected waves is shown in Fig. 6(a), clearly indicating that the transmission through such a structure is negligible, despite the fact that in contrast to the analytical predictions made for the continuous waves by the transfer-matrix approach, the beam has a finite frequency spectrum width. These results confirm that the zero-index gap is realistic, and it allows to suppress the transmission even for finite layered structures and for realistic parameters.

When the carrier frequency of the incident field is selected close to the resonant frequency of the defect mode, a significant amount of the energy is transmitted through the structure [see Fig. 6(b)]. Although the steady state of the transmission is not reached in the simulations and oscillations of the fields around the steady state continue at larger

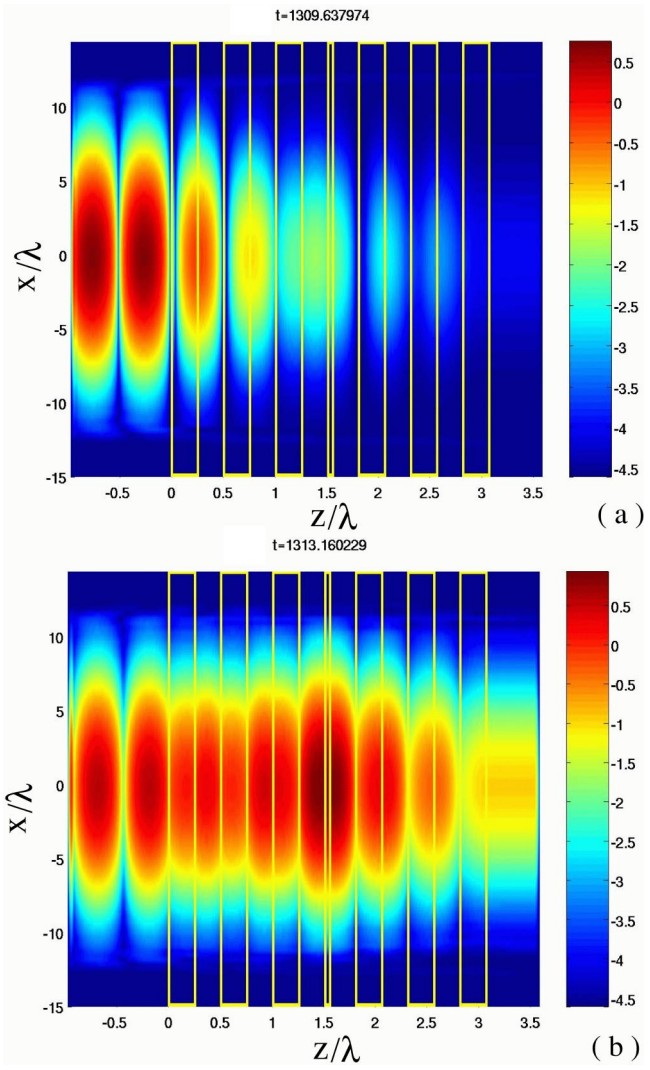

FIG. 7. (Color online). Results of the numerical FDTD simulations for the amplitude of the magnetic field in a two-dimensional structure (natural logarithm scale). Boxes show positions of the left-handed slabs, $a=0.25\lambda$, $\Delta=-0.8$. (a) Defect mode is not excited, $\omega=2\pi\times5.86\times10^9$ s^{-1}. (b) Defect mode is excited, $\omega=2\pi\times5.878\times10^9$ s^{-1}.

time scales, one can estimate the relaxation time of the resonance-induced transmission corresponding to the defect mode excitation time, which is found to be of the order of 10^3 periods (approximately 170 ns).

In Figs. 7(a) and 7(b) we show the examples of the field intensity distribution in the layered structure with the slab size $a=0.25\lambda$ for two distinct regimes of the beam transmission. In Fig. 7(a), the frequency corresponds to low transmission in Fig. 4(a), when no defect mode is excited. Figure 7(b) demonstrates the field distribution in the structure with an excited defect mode and enhanced transmission.

Based on the characteristic times of the relaxation processes in the beam transmission simulations, we can estimate the optimized time for the pulse propagation through the structure. Indeed, if the temporal pulse width is smaller than the relaxation time then the transmission should be low. Thus, in the pulse simulations, we consider the most crucial case when the pulse width is of the order of the relaxation time of the structure. Results of FDTD simulations for the pulse scattering from the multilayered structure with the period $a=0.25\lambda$ are presented in Figs. 8(a) and 8(b) as the temporal dependence of the incident, reflected, and transmitted energy flows. One can still clearly see, in spite of a relatively large relaxation time in the zero-index gap, a significant amount of the transmitted power, when the carrier frequency of the pulse coincides with the frequency of the defect mode.

V. CONCLUSIONS

We have studied, for the first time to our knowledge, the defect modes and transmission properties of periodic layered structures made of slabs of a left-handed metamaterial and air. Using realistic parameters of the metamaterial derived from the microscopic approach, we have calculated the band-gap spectrum of an infinite one-dimensional structure with and without structural defects, and demonstrated the existence of forbidden gaps of two different types, the conventional Bragg scattering gaps and a novel gap corresponding to the zero averaged refractive index $\langle n\rangle=0$.

We have analyzed the properties of the defect modes in a finite number of layers with a structural defect and demonstrated that, depending on the defect size, the defect modes

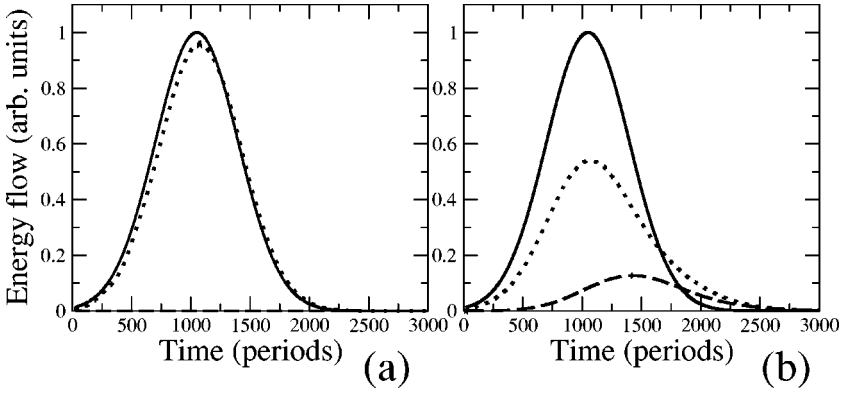

FIG. 8. Numerical FDTD simulation results for the pulse scattering by a periodic structure with defect. Solid: incident energy flow, dashed: transmitted energy flow, dotted: reflected energy flow. Parameters are $a=0.25\lambda$, $\Delta=-0.8$. (a) Defect mode is not excited, $\omega=2\pi\times5.86\times10^9$ s^{-1}. (b) Defect mode is excited, $\omega=2\pi\times5.878\times10^9$ s^{-1}.

appear in all or just some of the band gaps allowing to access different bandgaps selectively. In addition, we have performed two-dimensional numerical FDTD simulations of the propagation of electromagnetic waves in such structures and have studied the spatiotemporal dynamics of the beam transmission and reflection. We have demonstrated that the excitation of defect modes can enhance substantially the wave transmission through the structure, however, the excitation of the defect modes in the novel bandgap is characterized by relatively large relaxation time.

ACKNOWLEDGMENTS

The authors thank Dr. Michael Feise for fruitful collaboration and Professor Costas Soukoulis for useful discussions. This work has been partially supported by the Australian Research Council.

[1] V. G. Veselago, Usp. Fiz. Nauk **92**, 517 (1967) [Sov. Phys. Usp. **10**, 509 (1968)].
[2] R. A. Shelby, D. R. Smith, and S. Schultz, Science **292**, 77 (2001).
[3] C. G. Parazzoli, R. B. Greegor, K. Li, B. E. C. Koltenbah, and M. Tanielian, Phys. Rev. Lett. **90**, 107401 (2003).
[4] S. Foteinopoulou, E. N. Economou, and C. M. Soukoulis, Phys. Rev. Lett. **90**, 107402 (2003).
[5] Z. M. Zhang and C. J. Fu, Appl. Phys. Lett. **80**, 1097 (2002).
[6] I. S. Nefedov and S. A. Tretyakov, Phys. Rev. E **66**, 036611 (2002).
[7] J. B. Pendry and S. A. Ramakrishna, J. Phys.: Condens. Matter **15**, 6345 (2003).
[8] J. Li, L. Zhou, C. T. Chan, and P. Sheng, Phys. Rev. Lett. **90**, 083901 (2003).
[9] R. Ruppin, Microwave Opt. Technol. Lett. **38**, 494 (2003).
[10] I. V. Shadrivov, A. A. Sukhorukov, and Yu. S. Kivshar, Appl. Phys. Lett. **82**, 3820 (2003).
[11] L. Wu, S. L. He, and L. F. Shen, Phys. Rev. B **67**, 235103 (2003).
[12] J. B. Pendry, Focus Issue: Negative Refraction and Metamaterials, Opt. Express **11**, 639 (2003).
[13] T. J. Yen, W. J. Padilla, N. Fang, D. C. Vier, D. R. Smith, J. B. Pendry, D. N. Basov, and X. Zhang, Science **303**, 1494 (2004).
[14] J. B. Pendry, A. J. Holden, W. J. Stewart, and I. Youngs, Phys. Rev. Lett. **76**, 4773 (1996).
[15] A. A. Zharov, I. V. Shadrivov, and Yu. S. Kivshar, Phys. Rev. Lett. **91**, 037401 (2003).
[16] J. B. Pendry, A. J. Holden, D. J. Robbins, and W. J. Stewart, IEEE Trans. Microwave Theory Tech. **47**, 2075 (1999).
[17] L. D. Landau and E. M. Lifshitz, *Electrodynamics of Continuous Media* (Pergamon Press, Oxford, 1963).
[18] J. Schwinger, *Classical Electrodynamics* (Perseus Books, Reading, 1998).